Proc. Natl. Acad. Sci. USA
Vol. 95, pp. 13929–13934, November 1998
Neurobiology

Leading role of thalamic over cortical neurons during postinhibitory rebound excitation

F. GRENIER, I. TIMOFEEV, AND M. STERIADE*

Laboratoire de Neurophysiologie, Faculté de Médecine, Université Laval, Québec, Canada G1K 7P4

Communicated by Rodolfo R. Llinás, New York University Medical Center, New York, NY, September 18, 1998 (received for review March 30, 1998)

ABSTRACT **The postinhibitory rebound excitation is an intrinsic property of thalamic and cortical neurons that is implicated in a variety of normal and abnormal operations of neuronal networks, such as slow or fast brain rhythms during different states of vigilance as well as seizures. We used dual simultaneous intracellular recordings of thalamocortical neurons from the ventrolateral nucleus and neurons from the motor cortex, together with thalamic and cortical field potentials, to investigate the temporal relations between thalamic and cortical events during the rebound excitation that follows prolonged periods of stimulus-induced inhibition. Invariably, the rebound spike-bursts in thalamocortical cells occurred before the rebound depolarization in cortical neurons and preceded the peak of the depth-negative, rebound field potential in cortical areas. Also, the inhibitory-rebound sequences were more pronounced and prolonged in cortical neurons when elicited by thalamic stimuli, compared with cortical stimuli. The role of thalamocortical loops in the rebound excitation of cortical neurons was shown further by the absence of rebound activity in isolated cortical slabs. However, whereas thalamocortical neurons remained hyperpolarized after rebound excitation, because of the prolonged spike-bursts in inhibitory thalamic reticular neurons, the rebound depolarization in cortical neurons was prolonged, suggesting the role of intracortical excitatory circuits in this sustained activity. The role of intrathalamic events in triggering rebound cortical activity should be taken into consideration when analyzing information processes at the cortical level; at each step, corticothalamic volleys can set into action thalamic inhibitory neurons, leading to rebound spike-bursts that are transferred back to the cortex, thus modifying cortical activities.**

The postinhibitory rebound excitation is a cellular property used by thalamic and cortical neurons in a variety of normal and paroxysmal network operations, such as brain rhythms during various states of vigilance (1), intrathalamic (2) and intracortical (3) augmenting responses associated with short-term plasticity processes, and seizures in corticothalamic systems (4). In thalamocortical (TC) neurons, the rebound excitation is caused by a Ca^{2+}-dependent low-threshold spike (LTS), which is deinactivated by membrane hyperpolarization and can be crowned by high-frequency, Na^{+}-mediated fast-action potentials (5–7). The presence of the Ca^{2+}-dependent LTS was also shown in pyramidal and local-circuit cortical neurons (8, 9). Although the rebound excitation is an intrinsic property of both TC and cortical neurons, electrical stimuli applied to, or natural signals arising within, the thalamus or cortex produce a series of events that combine these two forebrain levels into a unified network. Thus, spindles and lower-frequency (delta and slow) oscillations occurring during quiescent sleep are characterized by prolonged periods of hyperpolarizations leading to rebound spike-bursts in three major neuronal classes: thalamic reticular (RE), TC, and neocortical neurons (1, 10–12). In addition, sensory volleys and synchronous electrical stimuli to the thalamus or cortex produce complex wave sequences caused by the interplay between the intrinsic properties of thalamic and cortical neurons and their reciprocal synaptic relationships. In this study, we used dual intracellular recordings from TC and cortical neurons, together with field potentials from the thalamus and cortex, to find the leading events in oscillations implicating postinhibitory rebound excitations. Data show that the postinhibitory rebound spike-bursts in TC cells prime the onset of rebound depolarizations in cortical neurons and that intact corticothalamocortical loops are necessary for the full development of rebound excitation in cortical neurons evoked by cortical stimuli.

METHODS

Experiments were conducted on 72 adult cats under either pentobarbital (35 mg/kg i.p.) or ketamine/xylazine (10–15 and 2–3 mg/kg i.m., respectively) anesthesia. The depth of anesthesia was monitored continuously by electroencephalogram (EEG). Additional doses of anesthetics were given when the EEG showed the slightest signs of activation (waves with lower amplitudes and higher frequencies). After the typical signs of deep anesthesia appeared on the EEG, the animals were paralyzed with gallamine triethiodide and artificially ventilated, and the end-tidal CO_2 was maintained at 3.5–3.7%. Heart rate was recorded (acceptable range was 90–110 beats per min), and body temperature was maintained at 37–39°C. As the animals were fixed in a stereotaxic apparatus, all pressure points were infiltrated generously with lidocaine. The stability of intracellular recordings was improved by inducing a bilateral pneumothorax, draining the cisterna magna, suspending the hip, and filling the hole made for recording with a solution of agar (4%).

Intracellular recordings of cortical neurons were performed from the precruciate motor area 4. For intracellular recordings from the ventrolateral (VL) and RE thalamic nuclei, the cortical surface corresponding to the anterior halves of the marginal and suprasylvian gyri was cauterized with silver nitrate and then removed by suction to reveal the head of the caudate nucleus. Micropipettes were lowered through the head of the caudate nucleus to reach the rostrolateral sector of the RE nucleus and the VL nucleus. Intracellular recordings were performed with glass micropipettes filled with 3 M potassium

The publication costs of this article were defrayed in part by page charge payment. This article must therefore be hereby marked "*advertisement*" in accordance with 18 U.S.C. §1734 solely to indicate this fact.

Abbreviations: EEG, electroencephalogram; EPSP, excitatory postsynaptic potential; GABA, γ-aminobutyric acid; LTS, low-threshold-spike; RE, thalamic reticular; STA, spike-triggered average; TC, thalamocortical; VL, thalamic ventrolateral; WTA, wave-triggered average.

*To whom reprint requests should be addressed. e-mail: mircea.steriade@phs.ulaval.ca.

acetate and DC resistances between 35 and 80 MΩ. The pipettes for intracellular recording in the cortex were placed ≈1 mm apart from the EEG electrode. The depth of the pipette was read from the micromanipulator. A high-impedance amplifier (bandpass of 0–5 kHz) with active bridge circuitry was used to record and inject current into the cells. The signals were recorded on an eight-channel tape with a bandpass of 0–9 kHz, later digitized at 20 kHz for off-line analysis. Recordings of field potentials were made with coaxial electrodes, with exposed areas of 0.1 mm separated by 0.6 mm. They were inserted in the lateral part of the precruciate gyrus area 4 for cortical recordings and stereotaxically in the VL nucleus for thalamic recordings. These electrodes were also used for stimulation. The distance between recording and stimulating electrodes in the cortex was 2 mm.

In some experiments (n = 14), a cortical slab was isolated from area 5 or 7 of the suprasylvian gyrus by using a homemade knife, but the pia mater was preserved. The slabs were ≈10 mm in the anteroposterior axis, ≈6 mm in the mediolateral axis, and ≈4–5 mm in depth. Further technical details of the slab preparation are given elsewhere (13).

All statistical values are given as mean ± standard error.

At the end of experiments, the animals were given a lethal dose of pentobarbital and perfused intracardially with physiological saline, followed by 10% formaldehyde. The completeness of slab isolation was verified on coronal sections (80 μm) stained with thionine.

RESULTS

The database consists of 187 TC cells from the VL nucleus, 25 RE cells from the rostrolateral sector, and 131 cortical cells from area 4. Of those recordings, we obtained 32 dual simultaneous impalements from VL and area 4 neurons. RE cells were identified by antidromic invasion from the dorsal thalamus (see Fig. 4) and could be distinguished from TC cells by their prolonged spike-bursts with typical accelerando-decelerando pattern, whereas TC cells displayed short

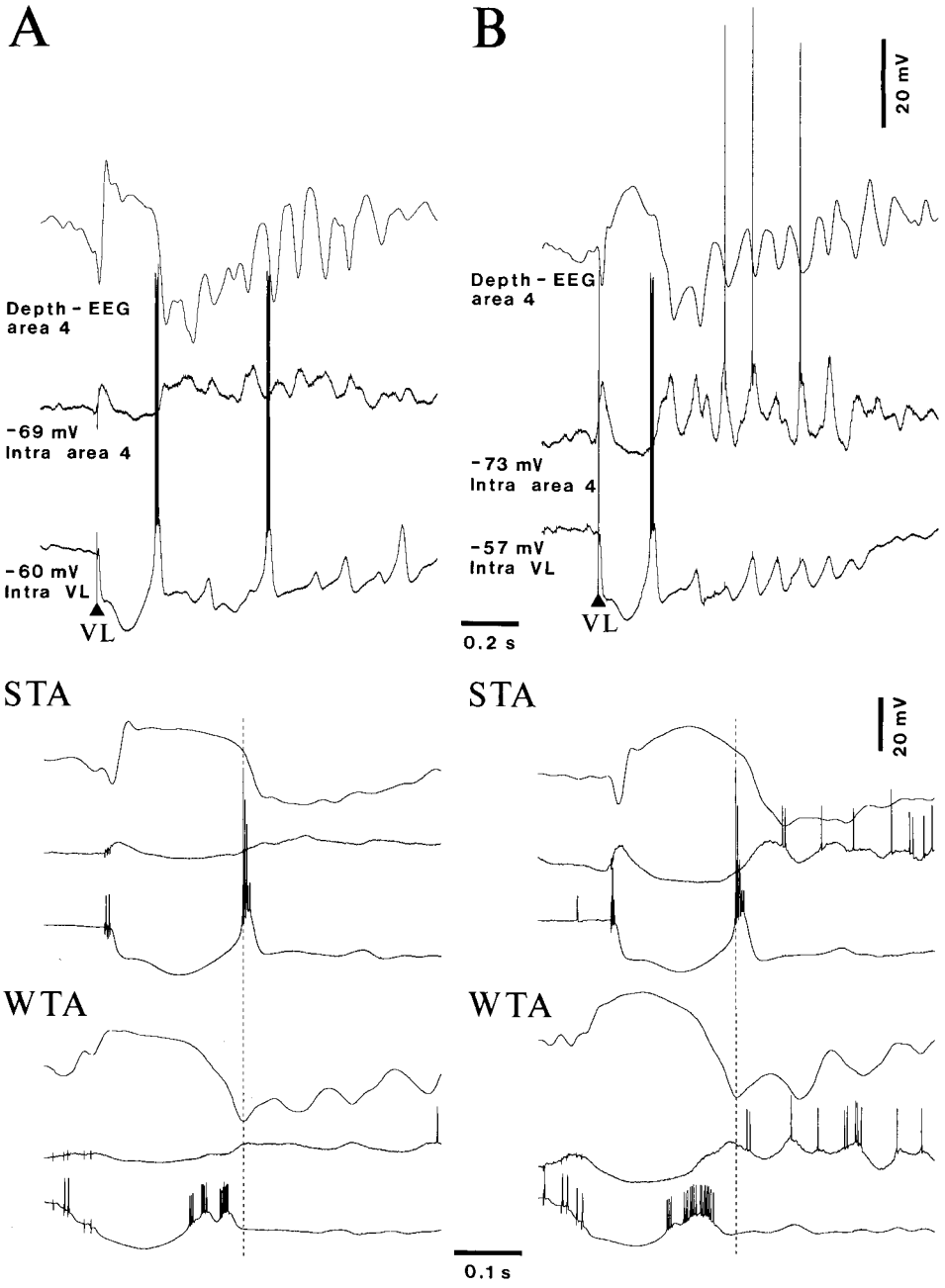

FIG. 1. Postinhibitory rebound spike-bursts elicited by VL stimulation in the TC neuron from the VL nucleus precede rebound activities in cortical area 4. Dual intracellular recordings from the same VL neuron and two area-4 neurons (*A* and *B*) are shown, together with field potentials from the depth of area 4. Recordings shown were made from cat under barbiturate anesthesia. (*Top*) Responses to single VL stimuli. (*Middle*) Corresponding spike-triggered averages (STA; n = 5) by first action potential in rebound spike-bursts of VL neuron. (*Bottom*) Wave-triggered averages (WTA; n = 5; same sweeps as for STA) by sharp depth-negative wave in area 4. The dotted line indicates reference time for both STA and WTA. Note that rebound spike-bursts in the VL cell preceded the cortical spindle sequence after stimulus-induced inhibition.

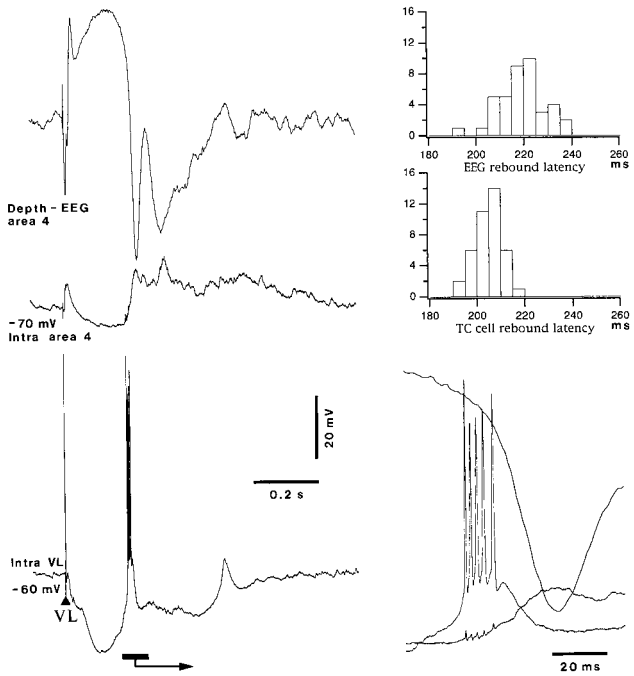

FIG. 2. Comparison between latencies of postinhibitory rebound in the VL neuron and field potential from the depth of area 4. Dual intracellular recordings from VL and area-4 neurons are shown, together with field potential from area 4. Recordings shown were made from cat under ketamine/xylazine anesthesia. (*Left*) VL stimulus elicits a postinhibitory rebound spike-burst in the VL cell followed by rebound depolarization in the area-4 neuron and depth-negative field potential in area 4. The rebound responses (marked by horizontal bar and arrow in *Lower Left*) are expanded in *Lower Right*; small deflections in intracellular recording from area 4 are caused by capacitive coupling from action potentials in the VL neuron. (*Upper Right*) Latency histograms of first action potential in rebound responses of the VL cell and peak negativity of field potential from area 4 ($n = 40$).

spike-bursts with progressively longer intervals between spikes (14). TC cells from the VL nucleus were backfired from area 4. The database of results obtained from isolated cortical slabs in 14 experiments consists of 72 cortical neurons from suprasylvian areas 5 and 7. The cells included in the database had stable membrane potential, below −55 mV for at least 20 min (up to 2 h), and overshooting action potentials.

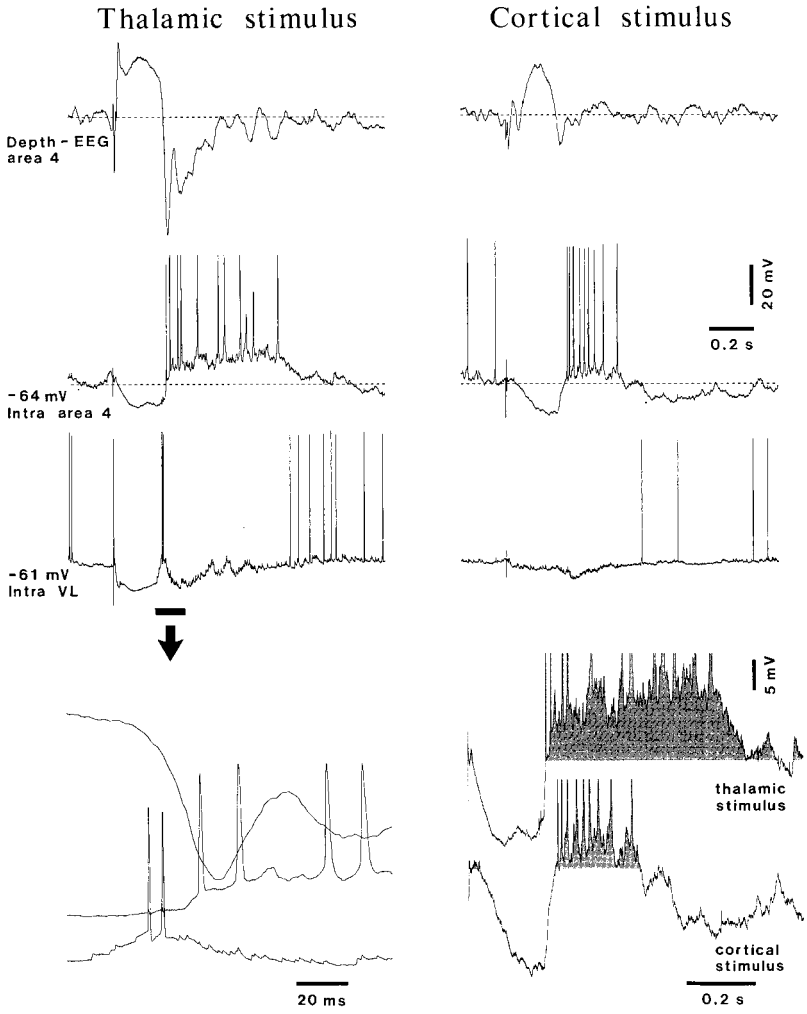

FIG. 3. Differential postinhibitory rebound responses elicited by thalamic and cortical stimulation. Dual intracellular recordings from VL and area-4 neurons (same in *Left* and *Right*) are shown, together with field potentials from the depth of area 4. Recordings shown were made from cat under ketamine/xylazine anesthesia. (*Top*) Stronger rebound response in the VL neuron to thalamic VL stimulation (compared with the response evoked in the same neuron by area-4 stimulation) correlates with longer-lasting and more ample postinhibitory depolarization in the area-4 neuron. Dotted lines in cortical recordings tentatively indicate the baseline. (*Bottom Left*) Part of the VL-evoked rebound response (indicated by an arrow) is expanded and shows that thalamic events precede cortical ones. (*Bottom Right*) Comparison of the thalamically and cortically evoked rebound depolarization in area 4 (dotted area over baseline).

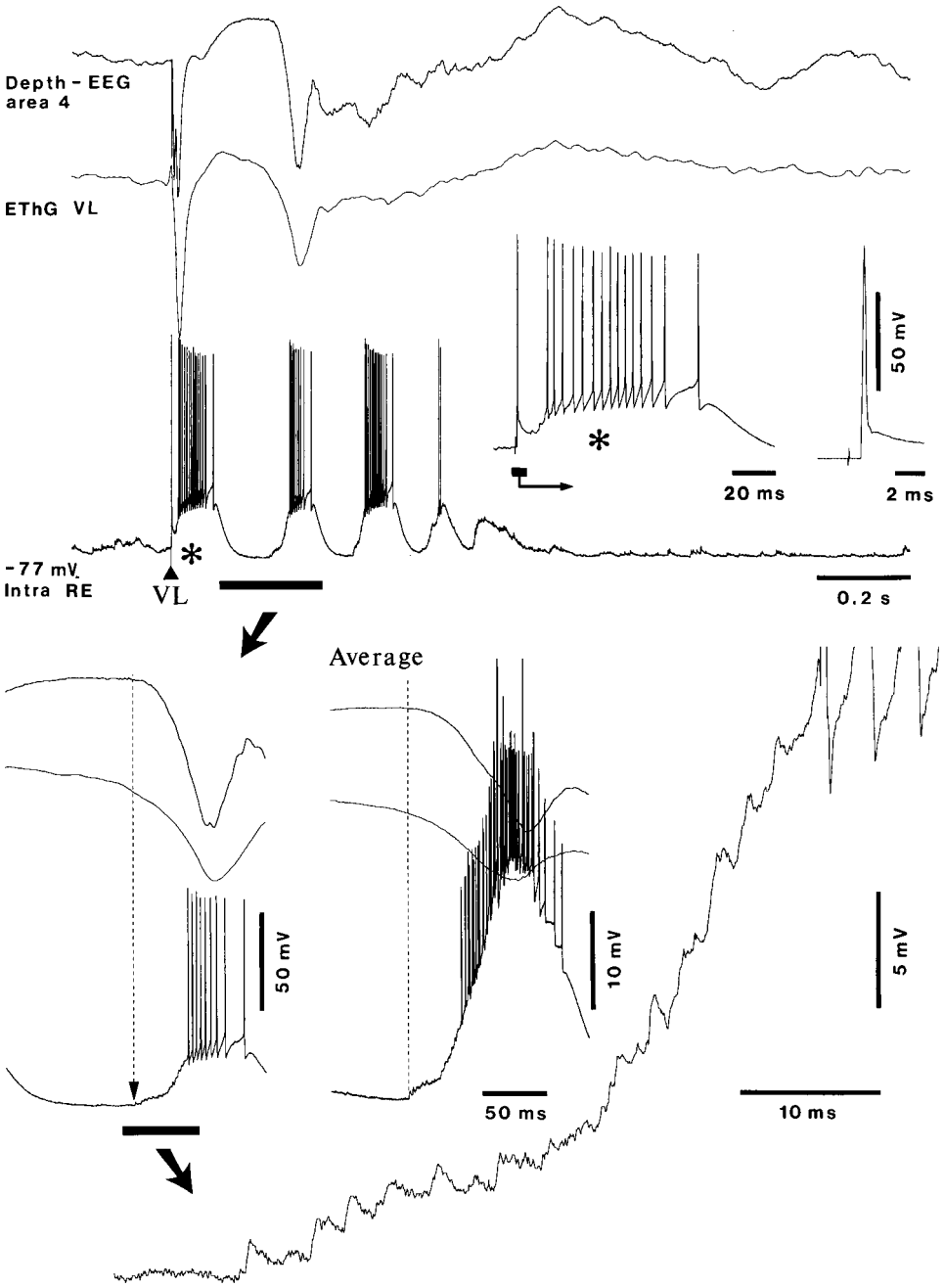

FIG. 4. Rebound EPSPs in the RE cell occur before rebound excitation in cortical area 4. Recordings shown were made from cat under ketamine/xylazine anesthesia. Intracellular recording of an RE cell from the rostrolateral sector of the RE nucleus is shown, together with field potentials from the VL nucleus and depth of area 4. (*Upper*) VL-evoked early response and spindle oscillation. (*Upper Right*) The early response in the RE neuron is expanded to show the initial antidromic discharge, followed by a high-frequency burst (indicated by an asterisk). (*Lower Left*) First postinhibitory excitation is expanded from the part marked by the horizontal bar and arrow in the *Upper* trace; the dotted line and arrow indicate the beginning of EPSPs in the RE neuron, well in advance of the onset of field negativity in area 4, but simultaneously with the developing rebound excitation in the field potential from the VL nucleus; below and to the right, RE-cell EPSPs are expanded further (as indicated by a horizontal bar and arrow). These EPSPs are triggered by rebound spike-bursts in TC cells (see text); EPSP-triggered average ($n = 5$) shows that EPSPs in the RE cell precede field negativity in area 4 (dotted line).

In cats studied under barbiturate anesthesia ($n = 42$), which produces prevalent spindling on the EEG, a single stimulus to the VL nucleus elicited a spindle sequence in TC cells. Of 109 TC cells recorded under barbiturate anesthesia, 63 displayed a rebound LTS crowned by a high-frequency spike-burst after the stimulus-elicited, long-lasting inhibitory postsynaptic potential. The biphasic inhibitory postsynaptic potential illustrated in Fig. 1 results from activation of γ-aminobutyric acid type A ($GABA_A$) and $GABA_B$ receptors (15, 16). In the simultaneously recorded cortical cells, the VL stimulus gave rise to a short-latency depolarization, and the postinhibitory rebound depolarization was shaped by the spindle sequence (Fig. 1 *A* and *B*). After their first rebound LTS, TC cells remained hyperpolarized, whereas cortical cells maintained a sustained depolarization (Fig. 1). The temporal relationship between the rebound LTS of TC cells and the rebound depolarization of simultaneously recorded cortical cells was assessed by using STA with reference to the first action potential in the rebound spike-burst of TC neurons and by using WTA with reference to the sharp depth-negativity of cortical field potentials. STA and WTA were calculated for five cell couples (TC and cortical). These analyses showed that the TC cell fired before the rebound depolarization of cortical cells associated with negative field potentials (Fig. 1). In all cases in which TC cells displayed action potentials superimposed on the stimulus-evoked rebound LTS, a similar temporal relation was found.

Basically similar relations between TC and cortical neurons were found when we used ketamine/xylazine anesthesia. After administering ketamine/xylazine, we analyzed the temporal relations between the rebound spike-bursts of TC cells and the depth-negative field potentials in area 4, reflecting summated depolarizations of deeply lying cortical neurons ($n = 7$). Fig. 2 depicts a dual intracellular recording from VL and area-4 neurons, together with the field potential from the depth of area 4. Latency histograms show that the rebound burst in the TC cell occurred about 14–15 ms before the peak of depth-negative cortical field potential. (Mean latencies were 205 ± 6

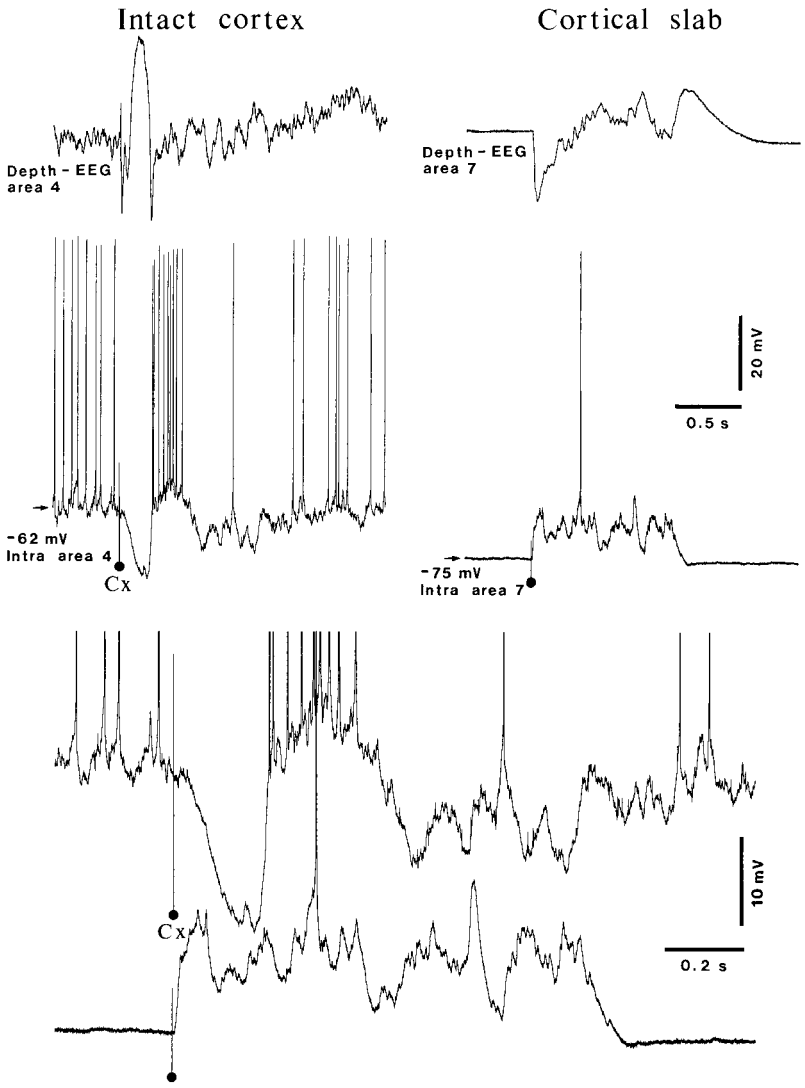

FIG. 5. Corticothalamic connections are essential for cortically evoked postinhibitory rebound excitation in cortical neurons. Intracellular recordings from two cortical neurons, one in an intact-brain animal, the other from an isolated cortical slab *in vivo*, are shown. Recordings shown were made from cats under ketamine/xylazine anesthesia. (*Top Left*) Inhibitory-rebound sequence in the neuron and field potential from the depth of area 4 evoked by area-4 stimulation. (*Top Right*) Responses in the neuron and depth field potential to stimulus applied in the isolated slab from cortical area 7. Note the absence of spontaneous activity in the area-7 slab. (*Bottom*) Responses are expanded to show an absence of inhibitory-rebound sequence in the isolated slab. Arrows indicate membrane potential in the intact cortex (−62 mV) and the isolated slab (−75 mV).

ms in the VL cell and 219 ± 10 ms in cortical field potential.) The paired comparison showed a highly significant difference ($P < 0.0001$). Note again that despite the initiation of rebound depolarization in the cortical neuron after the rebound spike-burst in the TC cell, the cortical neuron sustained a prolonged depolarization, whereas the TC neuron remained at a hyperpolarized level after its rebound LTS. Similar histograms were calculated for six TC cells and cortical field potentials. Although the mean of the delay between thalamic and cortical rebound activities varied for different TC neurons (range from 10 to 35 ms; mean 19.7 ± 1.3 ms), the rebound of TC cells significantly preceded the peak of cortical field potentials ($P <$ 0.0001, Student's paired t test).

We also investigated the difference between the effects induced by thalamic and cortical stimuli ($n = 12$). Fig. 3 (*Bottom Left*) shows that thalamic stimulation evoked an inhibitory-rebound sequence in the VL neuron whose rebound spike-burst was associated with the onset of cortical depth-negative field potentials and that this inhibitory-rebound sequence preceded the firing of the simultaneously recorded cortical neuron by ≈10 ms. Note the fast (≈50–100 Hz) excitatory postsynaptic potentials (EPSPs) in the VL cell, probably of cerebellar origin (17). Clearly, after the rebound LTS, the VL neuron remained hyperpolarized, whereas the area-4 neuron displayed a sustained depolarization for more than 0.5 s, events similar to those observed under barbiturate anesthesia (Fig. 1*A*). In contrast to the effect of thalamic stimulation, cortical stimuli elicited less pronounced inhibitory-rebound sequences in TC cells, less prolonged depolarizing rebound in cortical neurons, and, correlatively, smaller-amplitude depth-negative cortical field potentials (Fig. 3 *Right*). The mean duration of cortically evoked rebound in cortical neurons was measured under ketamine/xylazine anesthesia as 297 ± 34 ms ($n = 5$), whereas the duration of thalamically evoked rebound depolarization in cortical neurons under the same anesthesia was 536 ± 57 ms ($n = 7$).

In view of differences between TC and cortical neurons after the first inhibitory-rebound sequence (hyperpolarization vs. sustained depolarization, respectively; Figs. 1–3), we hypothesized that this contrasting aspect is caused by the rhythmic spike-bursts produced in GABAergic RE neurons by dorsal thalamic stimuli; consequently, the membrane potential of TC cells was maintained at a hyperpolarized level during the self-sustained spindle oscillation that follows a single dorsal thalamic stimulus. We analyzed this aspect in 25 RE neurons, recorded simultaneously with field potentials from the VL nucleus and cortical area 4. Indeed, VL stimulation induced (*i*) antidromic invasion of RE neuron, thus indicating that the RE cell projects to VL nucleus, followed by a prolonged spike-bursts, and (*ii*) after an inhibitory period, a spindle sequence consisting of rhythmic spike-bursts at ≈7–8 Hz (Fig. 4). This response was typical of those evoked in all investigated RE neurons. We compared the RE cell's response to thalamic and cortical field potentials evoked by the same stimulus and analyzed averaged activities with reference to the first barrages of EPSP leading to rebound spike-bursts in RE neurons ($n =$

6). Fig. 4 shows that barrages of EPSPs developed concomitantly with the negative field potential recorded from the VL nucleus and that these barrages are probably caused by the high-frequency spike-bursts of TC cells (18–20). However, the rebound spike-bursts fired by the RE neuron started before the peak negativity of the field potential recorded from the cortical depth. (The mean onset of the rebound spike-burst was at 28 ± 5 ms before the maximum of depth-negative cortical field potential.) This time relation corroborates the assertion that TC cells fire before the rebound depolarization in cortical cells. It also indicates that RE neurons are the probable source of sustained hyperpolarization observed in TC neurons, whereas the cortical neurons continue to develop a sustained depolarization.

Finally, because the data above pointed to the fact that rebound firing in TC cells precedes rebound depolarization in cortical neurons, we attempted to establish the essential role of TC neurons by comparing cortically elicited inhibitory-rebound sequences in intact brain and isolated cortical slabs from suprasylvian areas 5 or 7 ($n = 14$; Fig. 5). In the latter cases, all corticothalamocortical loops and long-range corticocortical connections were interrupted. As shown in Fig. 3, a cortical stimulus elicited a hyperpolarization-rebound sequence in the intact-brain preparation (Fig. 5 *Left*). The resting membrane potential of most of the neurons recorded in slabs was relatively hyperpolarized (below −70 mV). In contrast to the intact cortex, a cortical stimulus applied within the isolated slab elicited a long-lasting depolarization (1.6 ± 0.2 s) of cortical neurons ($n = 68$) consisting of both EPSPs and reversed inhibitory postsynaptic potentials but without a hyperpolarization leading to rebound activity.

DISCUSSION

The rebound spike-bursts of TC cells investigated in the present study follow prolonged periods of inhibition that are produced mainly by GABAergic RE neurons (1, 10–12), but also by local-circuit GABAergic cells especially in dorsal thalamic nuclei that are devoid of RE afferents (16). The inhibitory-rebound sequences explored here in the VL nucleus are characteristic for low-frequency oscillations of TC cells, such as those defining sleep spindles (1, 10–11). Other forms of TC rebound activities, with faster time courses and without typical high-frequency spike-bursts, having the propensity to develop fast oscillations, are generated preferentially at dendritic sites by activation of P/Q-type Ca^{2+} channels (21). Both long-lasting and short inhibitory periods leading to rebound activities in TC cells are projected to the cortex and, therefore, are implicated in low- and high-frequency brain rhythms. Although the hyperpolarization leading to rebound in TC cells is a biphasic, $GABA_A$- and $GABA_B$-mediated inhibitory postsynaptic potential (15, 16), the stimulus-elicited hyperpolarization in cortical neurons may be ascribed to both synaptic engagement of local-circuit inhibitory neurons (22) and to disfacilitation because of the concomitantly suppressed firing in TC neurons (23).

Our data show that the prolonged inhibitory-rebound sequences in TC neurons, typical for low-frequency sleep rhythms (10–12) and augmenting responses to repetitive (≈10-Hz) stimuli (2), precede the rebound depolarization in neocortical neurons. This temporal relation corroborates the results of recent experiments that used dual intracellular recordings from TC and cortical neurons and showed the priming role of spike-bursts in TC cells for the development of augmenting responses in cortical neurons (24). Importantly, however, although the rebound spike-bursts in TC cells initiate the rebound depolarization in cortical neurons, the depolarization is sustained in cortical neurons (Figs. 1–3) and, thus, is mainly attributable to intracortical (25), rather than TC, circuits. The mechanisms implicated in this sustained depolarization of cortical neurons are the activation of a persistent Na^+ current (26) and the reverberatory excitatory intracortical activity controlled by inhibition and activity-dependent synaptic depression (27–29).

The role played by intrathalamic events in initiating a cascade of cortical processes should be taken into consideration when successive intracortical steps are thought to underlie complex information processing exclusively. At each step, however, corticothalamic neurons impinge on both RE and TC cells, with obvious consequences in reentrant projections to the cortex. This dialogue between cortex and thalamus emphasizes the requirement of intact-brain preparations when the neuronal substrates of various functional states are investigated.

We thank P. Giguère and D. Drolet for technical assistance. F.G. is a Ph.D. student, partially supported by Fonds pour la Formation de Chercheurs et l'Aide à la Recherche. I.T. is a postdoctoral fellow, partially supported by the Savoy Foundation. This work was supported by grants from the Medical Research Council of Canada and Human Frontier Science Program.

1. Steriade, M., Jones, E. G. & Llinás, R. R. (1990) *Thalamic Oscillations and Signaling* (Wiley Interscience, New York).
2. Steriade, M. & Timofeev, I. (1997) *J. Neurosci.* **17,** 3778–3795.
3. Castro-Alamancos, M. & Connors, B. W. (1996) *J. Neurosci.* **16,** 7742–7756.
4. Steriade, M. & Contreras, D. (1995) *J. Neurosci.* **15,** 623–642.
5. Llinás, R. R. (1988) *Science* **242,** 1654–1664.
6. Jahnsen, H. & Llinás, R. (1984) *J. Physiol.* **349,** 227–247.
7. Deschênes, M., Paradis, M., Roy, J. P. & Steriade, M. (1984) *J. Neurophysiol.* **51,** 1196–1219.
8. Kawaguchi, Y. (1993) *J. Neurophysiol.* **69,** 416–431.
9. de la Peña, E. & Geijo-Barrientos, E. (1996) *J. Neurosci.* **16,** 5301–5311.
10. Steriade, M. & Llinás, R. R. (1988) *Physiol. Rev.* **68,** 649–742.
11. Steriade, M., McCormick, D. A. & Sejnowski, T. J. (1993) *Science* **262,** 679–685.
12. Steriade, M., Jones, E. G. & McCormick, D. A. (1997) *Thalamus: Organisation and Function* (Elsevier, Oxford), Vol. 1.
13. Timofeev, I., Grenier, F. & Steriade, M. (1998) *J. Neurophysiol.* **80,** 1495–1513.
14. Domich, L., Oakson, G. & Steriade, M. (1986) *J. Physiol.* **379,** 429–450.
15. Crunelli, V., Haby, M., Jassik-Gerschenfeld, D., Leresche, N. & Pirchio, M. (1988) *J. Physiol.* **399,** 153–176.
16. Paré, D., Curró Dossi, R. & Steriade, M. (1991) *J. Neurophysiol.* **66,** 1190–1204.
17. Timofeev, I. & Steriade, M. (1997) *J. Physiol.* **504,** 153–168.
18. Mulle, C., Madariaga, A. & Deschênes, M. (1986) *J. Neurosci.* **6,** 2134–2145.
19. Contreras, D., Curró Dossi, R. & Steriade, M. (1993) *J. Physiol.* **470,** 273–294.
20. Bal, T., von Krosigk, M. & McCormick, D. A. (1995) *J. Physiol.* **483,** 665–685.
21. Pedroarena, C. & Llinás, R. (1997) *Proc. Natl. Acad. Sci. USA* **94,** 724–728.
22. Contreras, D., Dürmüller, N. & Steriade, M. (1997) *J. Neurophysiol.* **78,** 2742–2753.
23. Contreras, D., Timofeev, I. & Steriade, M. (1996) *J. Physiol.* **494,** 251–264.
24. Steriade, M., Timofeev, I., Grenier, F. & Dürmüller, N. (1998) *J. Neurosci.* **18,** 6425–6443.
25. Jones, E. G. (1981) in *The Organization of the Cerebral Cortex*, eds. Schmitt, F. O., Worden, F. G., Adelman, G. & Dennis, S. G. (MIT Press, Cambridge, MA), pp. 199–235.
26. Stafstrom, C. E., Schwindt, P. C., Flatman, J. A. & Crill, W. E. (1984) *J. Neurophysiol.* **52,** 244–263.
27. Abbott, L. F., Varela, J. A., Sen, K. & Nelson, S. B. (1997) *Science* **275,** 220–224.
28. Varela, J. A., Sen, K., Gibson, J., Fost, J., Abbott, L. F. & Nelson, S. B. (1997) *J. Neurosci.* **17,** 7926–7940.
29. Turrigiano, G. G., Leslie, K. R., Desai, N. S., Rutherford, L. C. & Nelson, S. B. (1998) *Nature (London)* **391,** 892–896.